Interannual, Monthly, and Regional Variability in the Wet Season Diurnal Cycle of Precipitation in Sub-Saharan Africa

KAREN I. MOHR

Department of Earth and Atmospheric Sciences, The University at Albany, State University of New York, Albany, New York

(Manuscript received 21 August 2003, in final form 5 December 2003)

ABSTRACT

Convective systems in sub-Saharan Africa were defined from measurements by the Tropical Rainfall Measuring Mission satellite Microwave Imager at 85 GHz for four wet seasons, May–September 1998–2001. By applying a convective–stratiform discrimination algorithm to each convective system, the pixels within were designated as convective or stratiform cloud, life cycle ages assigned, and rainfall rates calculated. The years 1998 and 1999 were wetter than the long-term (1898–2000) mean, while 2000 and 2001 were drier. The wetter years had about 10% more convective systems than the drier years, but the size and intensity distributions for the wetter and drier years were virtually identical.

The wet season diurnal cycle of precipitation in the study area varied regionally, intraseasonally, and interannually. Analysis of precipitation versus time revealed different diurnal cycles for each of the three 10° zones south of the Sahara Desert. The diurnal cycle was bimodal north of 10°N and unimodal south of 10°N. The bimodal diurnal cycle was more pronounced north of 15°N. Diurnal cycles in each zone exhibited regional and seasonal variability of about 10% per four-hour time block. In wetter years the regional mean diurnal cycle was unimodal, but in drier years it was bimodal. The variability of the diurnal cycle appeared to be primarily influenced by variability in the frequency and life cycle of organized convective systems and thus the physical and dynamical factors responsible for their development.

1. Introduction

Dynamical weather/climate prediction models have had limited success in simulating the diurnal, seasonal, and annual cycles of precipitation in sub-Saharan Africa. One problem is that many processes and state variables controlling the interactions between the African land surface, the atmosphere, and the ocean are typically not well observed or described. Global studies of the diurnal cycles of the Tropics by Yang and Slingo (2001) and Nesbitt and Zipser (2003) note an early-morning peak in precipitation in sub-Saharan Africa, similar to the diurnal cycle of the tropical oceans. The principal hypothesis to explain this phenomenon is the life cycle of organized convective systems: that they originate in the late afternoon, reach their maximum extent, and then decay throughout the night.

In addition to temporal variability, precipitation in sub-Saharan Africa has significant spatial variability. The seasonal cycle drives the pronounced meridional gradient of precipitation from the Guinea Coast to the Sahara Desert. In a study of precipitation fluctuations during the 1980s, Nicholson (1993) acknowledges this gradient by dividing sub-Saharan Africa into 5 precipitation zones, approximately 3° in width. Within these zones, Hodges and Thorncroft (1997) find a potentially important source of variability, the propagation of organized convective systems away from favored initiation locations. From the 1992 Hydrological–Atmospheric Pilot Experiment-Sahel (HAPEX-Sahel) surface observations, Taylor and Lebel (1998) detected mesoscale precipitation gradients that persisted from a few days to a month. They mention frequency of convective system passage and a positive land–atmosphere feedback as mechanisms for this phenomenon. Because the seasonal cycle and highly variable environmental conditions influence the development of convective systems in sub-Saharan Africa, the diurnal cycle of precipitation would also be dynamic, possessing both temporal and spatial variability on a variety of scales.

There is a gap in the African climate literature between studies of interannual variability of convection such as Desbois et al. (1988) and Mathon et al. (2002) and studies diagnosing the diurnal cycle (e.g., Rowell and Milford 1993; Shinoda et al. 1999). Global studies such as Yang and Slingo (2001) and even the regional studies cited previously diagnose a single African diurnal cycle. Shinoda et al. (1999) make one additional distinction, diurnal cycles during wetter than average versus drier than average years. Global studies neces-

Corresponding author address: Karen I. Mohr, Department of Earth and Atmospheric Sciences, The University at Albany, SUNY, Albany, NY 12222.
E-mail: mohr@atmos.albany.edu

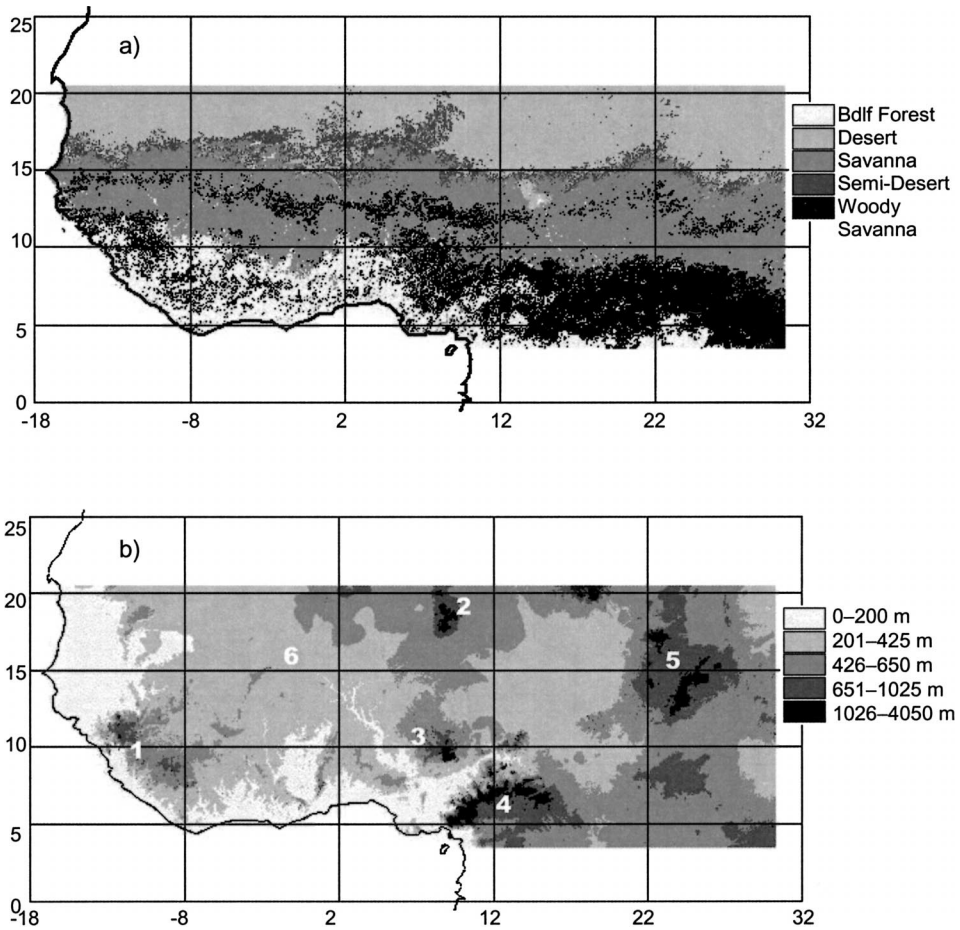

FIG. 1. (a) Land cover in the study area, approximately 3°–21°N, 17°W–30°E; Bdlf ≡ broadleaf. (b) Topography in the study area. Scale is not linear. Areas of significant relief: 1–Guinea Highlands, 2–Aïr Mountains, 3–Jos Plateau, 4–Cameroon Highlands, 5–Dhafur Mountains. The northern branch of the Niger River is at 6.

sarily cannot examine regional or temporal variations in detail. This study explores the links between convective variability and the diurnal cycle in sub-Saharan Africa, using a database that covers seasonal and/or interannual variations in the diurnal cycle over the entire region west of the Ethiopian highlands and south of the Sahara Desert, a larger area and/or longer time period than previous efforts.

The Tropical Rainfall Measuring Mission (TRMM) satellite was launched in 1997 to provide high-resolution observations of rainfall and related variables in the Tropics. The TRMM data for four wet seasons (May–September) 1998–2001 is used to define and analyze the diurnal cycle in the study region. The diurnal cycle of precipitation in sub-Saharan Africa is a particularly poorly simulated feature by dynamical models. Documenting changes in the diurnal cycle with respect to time and space should advance the body of work describing the key physical processes involved in African precipitation cycles.

2. Background

Maps of the study area are in Fig. 1. Figure 1 was derived from U.S. Geological Survey land cover classification maps of the region available from the Africa Data Dissemination Service (available online at http://edcsnw4.cr.usgs.gov/adds/index.php). The grid between 5° and 20°N contains 15 latitude–longitude boxes, and there are three zones, each 5° in width, that contain a predominant land cover. The zone north of 15°N contains semidesert and desert biomes. Between 15° and 10°N, the land cover is principally savanna. Savanna with a high proportion of trees and woody shrubs is termed ''woody savanna'' (Bailey 1998). Patches of woody savanna occur in the middle zone, but in the zone south of 10°N, the woody savanna is continuous. In this coastal zone, particularly west of 5°E, evergreen broadleaf forest naturally occurs. The land cover classifications in Fig. 1 make no distinction between degraded and old-growth broadleaf forest, and the text will

refer to this zone containing both broadleaf forest and woody savanna as ''forest.'' The layout of land cover in sub-Saharan Africa makes it possible to compare land cover zones of roughly the same size.

Because the area in Fig. 1 is large and does not have a dense, organized ground-observing network, remote sensing is frequently used to conduct regional studies of convection and precipitation. The studies by Duvel (1989), Machado et al. (1992, 1993), Laing and Fritsch (1993), Hodges and Thorncroft (1997), and Mathon and Laurent (2001) use IR remote sensing while the studies of Mohr et al. (1999), Nesbitt et al. (2000), and Peterson and Rutledge (2001) use microwave remote sensing. In both sets of studies, large, organized convective systems are an important feature of the wet season hydrologic cycle in sub-Saharan Africa. Large convective systems contribute more to regional cloud cover and precipitation than their share of the convective system population, although the contribution attributed to organized convective systems is higher in the IR studies than in the microwave studies.

Differences in the physics of IR and microwave remote sensing complicate the comparison of results between studies using the other technique. Nonraining anvil tops may be much larger than precipitating cloud, and very cold cloud-top temperatures may be observed long after active convection has peaked in intensity or even ceased. Toracinta et al. (1996) have several examples of the latter phenomenon. It is entirely possible, if not probable, that some organized convective systems with very cold cloud tops observed by IR sensors are much smaller and weaker systems when analyzed using microwave retrieval techniques. Over time and space, differences in system classification by IR and microwave-based retrieval schemes would lead to discrepancies in calculated precipitation contributions with respect to system size. Conceivably, this would also affect the derivation of the diurnal cycle, especially in the early morning since decaying systems are most likely to be analyzed differently. Because microwave remote-sensing techniques can more accurately distinguish between raining and nonraining cloud, the study database is developed from TRMM Microwave Imager (TMI) measurements.

3. Data and methods

a. Processing of TRMM data products

From November 1997 to late August 2001, the TRMM satellite flew at an altitude of approximately 350 km. The satellite was raised to an altitude of approximately 402 km to extend its operational lifetime. The original altitude permitted TRMM to precess through the diurnal cycle at a given geolocation in 46.4 days. After August 2001, the precession through the diurnal cycle increased slightly to 47.5 days. Kummerow et al. (1998) provide details on the complete instrument package on TRMM. This study uses orbital data products (1B11) from the TMI dual-polarized 85.5-GHz channel. The 1B11 data product is ungridded, thus preserving the sensor resolution (4.6 km $\times$ 6.95 km). At TRMM's original altitude, the TMI swath was 759 km wide. Both the swath width and the sensor footprint increased slightly after the altitude boost in August 2001. Because a very small percentage of the study data occurred after the altitude boost, all data are treated as if they have essentially the same resolution.

Negri et al. (2002) conducted a detailed study of the potential biases in constructing the diurnal cycle of precipitation by TRMM for the Amazon basin. The spatial–temporal resolution of the analysis in this study was based on their conclusions. Negri et al. conclude that eliminating hourly variations in the TMI sampling pattern requires the accumulation (or averaging) over 4 h of local time. For a 5° $\times$ 5° box, Negri et al. found sampling errors for the TMI to be on the order of 10%. This study uses 4-h accumulation and, in the analysis of diurnal cycles, limits the use of the 10° meridional segments in Fig. 1 to assessing regional variability.

The surface emissivity at 85.5 GHz can vary with land surface type (e.g., water, sand, moist or dry vegetation) for TMI's oblique viewing angle (49°). Spencer et al. (1989) use differences in the polarization of the radiation emitted from the heterogeneous surface to derive a polarization-corrected temperature (PCT). The PCT mostly eliminates emissivity discontinuities due to the surface type.

$$\mathrm{PCT}_{85} = 1.8 \times \mathrm{T85}_V - 0.8 \times \mathrm{T85}_H \qquad (1)$$

The $\mathrm{T85}_V$ and $\mathrm{T85}_H$ refer to the vertically and horizontally polarized 85-GHz brightness temperatures. Mohr and Zipser (1996) and Nesbitt et al. (2000) successfully use the PCT to identify convective systems and compare differences in intensity between land-based and ocean-based systems. The PCT will be applied in a similar manner to analyze convective system properties in this study.

All 85-GHz TMI data from all TRMM orbits over the study area for May–September 1998–2001 were converted to PCT and then processed through a pattern-recognition algorithm. The algorithm identified all contiguous pixels with PCTs less than or equal to a contour PCT of 255 K. This contour temperature was chosen for consistency with the convective/stratiform discrimination algorithm described in the next section. The time and date of the TRMM overpass, cloud cluster location, cloud cluster size, and a histogram of the PCTs of the pixels were recorded for each cloud cluster and then stored in a relational database. Only cloud clusters whose centroids were located over land were retained in the database and then subjected to the convective–stratiform discrimination algorithm. After the application of the second algorithm, the areas and rain rates of each cloud type were added to the database.

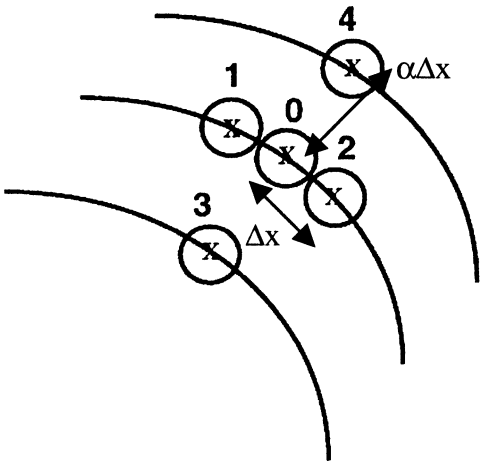

FIG. 2. The solid curves are the conical scan of the TMI radiometer, and the circles (pixels) are the footprints. The pixel 0 represents $T85_{min}$. The spatial gradients are calculated using the pixels numbered 1–4 around pixel 0. The distance Δx between the centers (X) of consecutive pixels on the same scan is 4.6 km. The distance $\alpha\Delta x$ between pixels in the same position but on different scans is 13.9 km where $\alpha = 3.02$. Adapted from Fig. 2 in PIWD.

b. Convective–stratiform discrimination algorithm

The 4.6 km $\times$ 6.95 km resolution of the TMI makes it possible to perform convective-scale analysis on cloud lines and clusters. Prabhakara et al. (2000), henceforth referred to as PIWD, developed a convective–stratiform discrimination algorithm that uses horizontal gradients of T85 to identify individual cumulonimbus clouds (Cbs) within an area of depressed brightness temperatures. Pixels not associated with Cbs are classified as stratiform cloud.

Using TRMM precipitation radar (PR) and TMI scans of the same mesoscale convective systems (MCSs), PIWD show that local minima in T85 correspond roughly to maxima in the PR rain map. The local minima in T85 represent Cbs. A local minimum, $T85_{min}$, occurs whenever the central pixel of three consecutive pixels on the same TMI scan is colder than the pixels to its east and west. In Fig. 2, the pixel numbered "0" is classified as $T85_{min}$ if and only if it is colder than pixels 1 and 2. By calculating the mean of the absolute values of the T85 gradients $|\overline{dT85/dr}|$ around each Cb, they could infer the spatial structure and type of hydrometeors most likely to be producing the ice-scattering signature around $T85_{min}$. The T85 gradient is calculated as follows:

$$\left.\overline{\frac{dT85}{dr}}\right|_{5\,pt} = \frac{1}{4}\Delta x(T85_1 + T85_2) + \frac{1}{4}\alpha\Delta x(T85_3 + T85_4) - \frac{(\alpha + 1)T85_0}{2\alpha\Delta x}. \quad (2)$$

Figure 2 illustrates the position of pixels numbered 1–4 relative to $T85_{min}$ (pixel 0). The average distance between pixel centers on the same scan (Δx) is 4.6 km, and $\alpha\Delta x$ is the distance, 13.9 km, between pixels on different scans with the same scan position. In a further modification to the original PIWD algorithm, a T85 gradient is also calculated from pixels 0–2 (R. Iacovazzi 2002, personal communication) as follows,

$$\left.\overline{\frac{dT85}{dr}}\right|_{3\,pt} = \frac{1}{2}\Delta x(T85_1 + T85_2 - 2T85_0). \quad (3)$$

The larger of the two T85 gradients, 3 points and 5 points, becomes the representative T85 gradient around $T85_{min}$. In Table 1 are the criteria PIWD developed that use the T85 gradient and $T85_{min}$ to distinguish among convectively active young, mature, and decaying Cbs. Using the information from the PR, PIWD derive an average rain rate for each class of Cb. The rain rates listed in Table 1 represent the average rain rate of pixels 0–4. Those pixels not associated with a Cb are assigned the stratiform rain rate.

In Figure 3 the locations of Cbs are superimposed over the contour plots of PCT for representative convective systems. Note that many of the plus (+) signs indicating young Cbs are on the edges of the cloud shield where outflow from older Cbs is triggering new Cbs. A large number of plus signs occur within the cloud shield. In the numerous contour plots (not shown) generated in the course of the research, this is a common phenomenon. It appears that the PIWD criteria for a young Cb do not produce a unique solution because two different fields of hydrometeors above the freezing level could produce the same T85 gradient: 1) a mixture of

TABLE 1. Classification of convective and stratiform cloud using $T85_{min}$ and the T85 gradient. Rain-rate coefficients are derived empirically in PIWD.

Cloud type	T85 gradient	85-GHz minimum	Rain rate (mm h^{-1})
Young Cb	$\overline{\frac{dT85}{dr}} > 1$ K km^{-1}	255 K $>$ $T85_{min}$ $>$ 210 K	$0.25(255 - T85_{min})$
Mature Cb	$\overline{\frac{dT85}{dr}} > 1$ K km^{-1}	$T85_{min} < 210$ K	$11.25 + 0.35(210 - T85_{min})$
Decaying Cb	$\overline{\frac{dT85}{dr}} < 1$ K km^{-1}	255 K $>$ $T85_{min}$	$0.12(255 - T85_{min})$
Stratiform	N/A	N/A	$0.12(260 - T85_{min})$

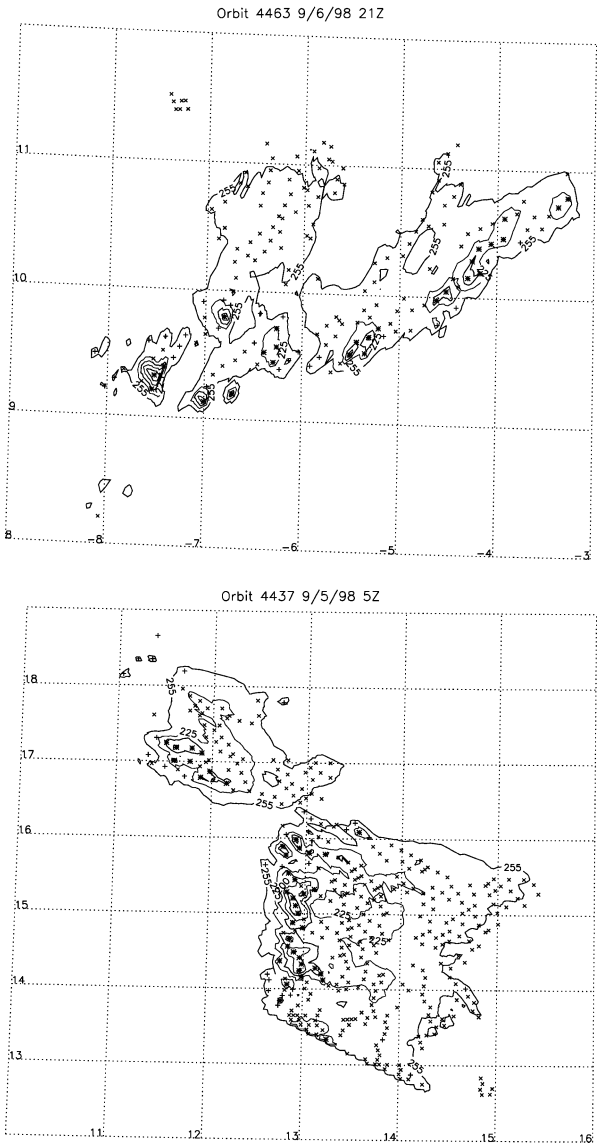

FIG. 3. Contour plots of T85 for two TRMM overpasses in Sep 1998. Mature Cbs are indicated with asterisks (*), young/weak Cbs with plus signs (+), and decaying Cbs with crosses (×). Some Cbs are uncontoured because they are below the resolution of the contouring software.

graupel, snow, and cloud ice with a significant volume of supercooled water that would be typical of new convection, and 2) a mixture of snow and cloud ice, with a small volume of graupel that could occur in mature, but weak, convection. Hence, the PIWD ''young'' classification will be amended to a ''young/weak'' classification. The mature Cbs invariably coincide with the coldest ice-scattering cores, and decaying Cbs appear in the expected places as well. The PIWD convective–stratiform discrimination algorithm appears to be a useful first-order classification for cloud clusters and lines identified from 85-GHz ice-scattering features.

4. Diagnosis of selected population characteristics 1998–2001

a. Geographic distribution

The Joint Institute for the Study of the Atmosphere and Ocean at the University of Washington, Seattle, displays plotted time series of African precipitation indices (available online at http://tao.atmos.washington.edu/data_sets/). West Africa demonstrates decadal-scale variability in regional precipitation, with the years since the late sixties constituting a dry period (time series not shown). Some higher-frequency variation is observed. In the West African Sahel (northern third of the study area), the years 1998 and 1999 are wetter than the long-term mean (1898–2000) whereas the years 2000 and 2001 are drier than the long-term mean. In the Gulf of Guinea region (southern third of the study area), 1999 is wetter than the long-term mean, and 2000 and 2001 are drier. Although 1998 is drier than the long-term mean it has a smaller negative anomaly than 2000 and 2001. In the context of the recent dry trend, the study database covers two wetter years and two drier years.

The convective systems in the study database were sorted into boxes by latitude and longitude. In Fig. 1a, the width of the savanna and forest biomes is approximately 5°. In Fig. 4, for each year in the database (1998–2001), the number of clusters observed in each box was divided by the total number of systems observed. The percentages for all 4 yr are plotted in each box (1998 and 1999 on the top line, 2000 and 2001 on the bottom line) to facilitate year-to-year comparisons. The percentages plotted in Fig. 4 correspond to the zonal layout of the major biomes in Fig. 1a and a meridional decrease in vegetation density. The geographic distribution of convective systems is essentially the same during the wetter years 1998 and 1999 and the drier years 2000 and 2001. There are no pronounced directional shifts (northward, eastward, etc.) of the convective system population between the wetter and drier years.

b. Size and intensity distributions

Table 2 contains the total number of convective systems detected by TRMM for each year in the database and the number of convective systems in each age/intensity category. The age/intensity categories were assigned to each convective system using the PIWD algorithm. Mature systems had at least one mature Cb. Young/weak systems had no mature Cbs and at least one young/weak Cb. Systems that met neither of these criteria were assigned to the decaying/stratiform category. In the far right-hand column of Table 2 is a comparison of the two wetter years (1998 and 1999) and the two drier years (2000 and 2001). The two wetter years had on the order of 10% more convective systems detectable by TRMM than the drier years. Because TRMM makes discrete observations, it is not possible

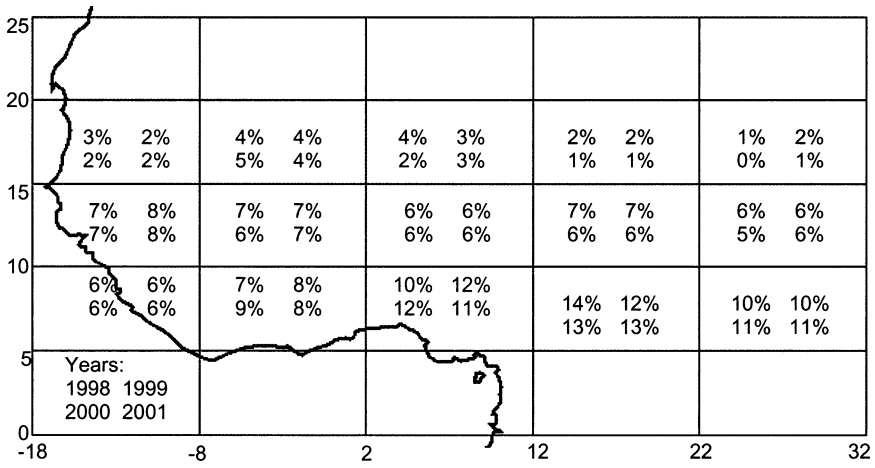

FIG. 4. Geographic distribution of convective systems for 1998–2001. The number of convective systems observed in each box was divided by the total number of systems observed that year in the study area. Only land-based systems were counted in boxes straddling the coast. Percentages do not add up to 100% because a few systems in the database were observed south of 5°N or north of 20°N. Years 1998 and 1999 are plotted on the top line, 2000 and 2001 on the bottom line.

to say how many convective systems changed age/intensity categories afterward. Even if the geographic distributions of convective systems were stable for 1998–2001 (Fig. 4), the actual numbers of convective systems did indeed vary from year to year (Table 2) in each latitude–longitude box.

More precipitation would occur in wetter years if convective systems were larger and/or more intense in wetter years. Figure 5 is a series of cumulative frequency distributions for (a) total system area for all convective systems, (b) area of mature Cbs, (c) area of decaying Cb/stratiform cloud, (d) average PCT of mature Cbs in mature convective systems. Figures 5b,d were calculated using mature convective systems only, and Fig. 5c represents all convective systems having the applicable cloud types. In all of the graphs in Fig. 5, the distributions lie on top of each other. There is no statistically significant difference in the size or intensity characteristics of the convective system population between the wetter (1998, 1999) and drier (2000, 2001) years. The range of sizes and average PCT is the same as well. There are 10% more convective systems with a total system area greater than 1000 km^2, but large convective systems constitute the same fraction of the population in the wetter years as they do in the drier years. From Figs. 4 and 5 and Table 2, the only difference between the two wetter and two drier years observed by TRMM is the frequency of occurrence of convective systems. It appears that the years 1998 and 1999 had more precipitation than 2000 and 2001 because more convective systems developed and not because they tended to be bigger and/or more intense.

c. Contribution to precipitation from organized convective systems

Previous studies using IR or microwave remote sensing have emphasized the contribution to precipitation in sub-Saharan Africa from organized convective systems. A wetter year will have a higher frequency of organized convective systems than a drier year. For the purposes of this paper, the term *organized convective system* refers to convective systems that have at least four mature Cbs and reach the 90th percentile for total system size and/or the 10th percentile for lowest average PCT of mature Cbs. To reach such a large size or cold average PCT, dynamic and thermodynamic interactions among multiple Cbs in various life cycle stages would

TABLE 2. Convective systems detectable by TRMM in the study area. The ''wet vs dry'' column is the percent difference in system frequency between the two wetter years (1998 and 1999) and the two drier years (2000 and 2001).

System type	1998	1999	2000	2001	Wet vs dry
Young/weak	13 277	14 983	12 327	12 062	14%
Mature	5531	6111	5598	5138	8%
Decaying/stratiform	2525	2793	2398	2382	10%
Total	21 333	23 887	20 323	19 582	12%
Overpasses	1330	1332	1332	1439*	

* Altitude boost in Aug 2001.

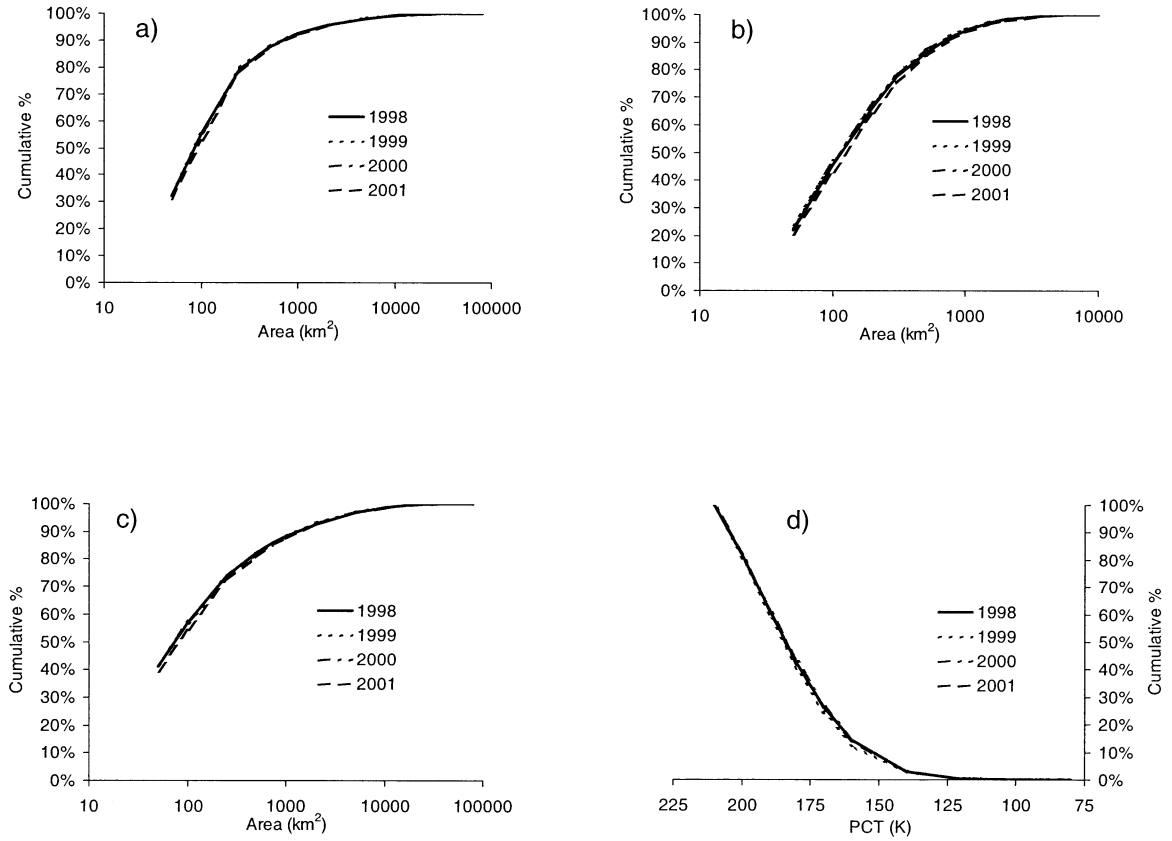

FIG. 5. Cumulative frequency distributions for (a) total system area (all convective systems), (b) area of mature Cbs, (c) area of decaying Cb/stratiform cloud, (d) average PCT of mature Cbs in mature convective systems.

be required, hence the adjective ''organized.'' In the cumulative frequency distributions in Fig. 5, the 90th percentile for total system size is approximately 1000 km^2, and the 10th percentile for average PCT of mature Cbs is approximately 150 K. A convective system was classified as organized if it was greater than 1000 km^2 or had four or more mature CBs with an average PCT colder than 150 K or both. Of all the convective systems meeting one or more of the criteria, about 45% met the size but not intensity criterion, 40% met the intensity but not size criterion, and 15% met both criteria. The convective systems meeting both criteria were counted only once.

Table 3 is the contribution to total precipitation for each month by organized convective systems. The volumetric rainfall (mm h^{-1} km^2) contribution from each convective system was based on the PIWD algorithm in Table 1. The contributions were summed for each latitude–longitude box (Fig. 1). Except for May, organized convective systems contribute a greater share of the precipitation in the savanna zone (10°–15°N) than in the semidesert (>15°N) or forest (<10°N) zones. Conversely, the forest zone has the lowest zonal average contribution from organized convective systems June–September. The progression of the ITCZ ensures that the northernmost semidesert zone has the largest seasonal variability with respect to organized convective systems. In the semidesert zone, the contribution by organized convective systems ranges from 34% in May to 74% in August. In August, the peak of the wet season in the semidesert zone, the 74% is an average of individual boxes ranging from 46% (>22°E) to 83% (>8°W). Across the savanna zone, the contribution from organized convective systems varies from 1%–15%, less than half the zonal variability of the semidesert. Zonal variability in the forest is lowest in May and June (<10%), and highest in July and August (<20%).

Precipitation contributions from organized convective systems are 10%–15% higher in the savanna than in the forest. Figure 6 reveals two possibilities for this difference. In June and September, the forest had 40% more convective systems and 30% more organized convective systems than the savanna, but the organized convective systems comprised only 8% of the forest convective system population compared to 12% in the savanna. In July and August, the forest has 10% fewer organized convective systems even though it has 20% more convective systems than the savanna. The organized convective systems comprise only 6% of the forest convective system population versus 10% in the savanna. Even when there are fewer organized convective systems in the savanna, they remain a larger share of its

TABLE 3. Percent of total precipitation for 1998–2001 contributed by organized convective systems. Land cover in the >15°N zone is semidesert, 10°–15°N savanna, <10°N forest.

	<8°W	8°W–2°E	2°–12°E	12°–22°E	>22°E	Zone
May						
>15°N	28%	26%	24%	39%	52%	34%
10°–15°N	60%	64%	76%	64%	58%	66%
10°N>	71%	68%	77%	74%	73%	74%
Jun						
>15°N	58%	58%	40%	40%	67%	53%
10°–15°N	84%	82%	85%	77%	70%	81%
10°N>	72%	68%	77%	69%	70%	72%
Jul						
>15°N	73%	72%	62%	50%	52%	66%
10°–15°N	76%	81%	82%	80%	71%	79%
10°N>	53%	48%	58%	67%	65%	62%
Aug						
>15°N	83%	75%	74%	65%	46%	74%
10°–15°N	76%	73%	83%	81%	70%	77%
10°N>	52%	60%	63%	67%	64%	64%
Sep						
>15°N	81%	73%	51%	78%	71%	73%
10°–15°N	82%	80%	83%	83%	81%	82%
10°N>	67%	65%	71%	70%	71%	70%

convective system population compared to the other zones.

5. Variability of the diurnal cycle

Global studies Yang and Slingo (2001) and Nesbitt and Zipser (2003) derive a regional composite diurnal cycle for sub-Saharan Africa, leaving the task of finding subregional variations to smaller-scale studies. The distributions in Fig. 7 were compiled from all convective systems in the study database, and 4-h local time blocks were established to reduce temporal sampling bias from TRMM (Negri et al. 2002). Figure 7a depicts the typical continental diurnal cycle, with a peak in convective activity between 1400–1800 local time (LT). Subtle monthly differences are apparent. A higher percentage of May and August convective systems were observed in the 1400–1800 LT block than in June, July, and September. Conversely, May and August have the fewest late-night/early-morning convective systems. The peaks in convective activity (Fig. 7a) and precipitation (Fig. 7b) do not coincide. As in Fig. 7a, there are noticeable monthly differences in Fig. 7b. Precipitation peaks in the 1800–2200 LT block for May and August compared to the 2200–0200 LT block in June and the 0200–0600 LT block in July and September. The fraction of precipitation in the two time blocks covering 2200 to 0600 LT is higher in June, July, and September than in May and August.

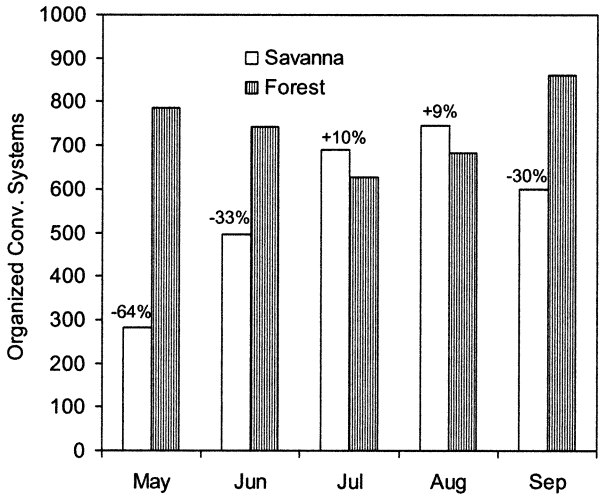

FIG. 6. The number of organized convective systems occurring in the savanna (10°–15°N) and forest (south of 10°N) zones by month for 1998–2001. The labels above the savanna series bars are the percent difference between the savanna and forest.

Figure 8 contains the mean wet season diurnal cycle of precipitation for each of the zones of this study: the semidesert zone (>15°N), savanna zone (10°–15°N), and forest zone (<10°N). For each zone, the diurnal cycle is in the form of a high–low graph where the zonal mean is plotted as a square with vertical bars stretching from the lowest value to the highest value. The means were calculated from the percent of total precipitation in each longitude box (five values) for the entire wet season, and the high–low bars were derived from the maximum and minimum values in the five boxes across the zone. The high–low bars depict the variability of the diurnal cycles within each zone. From north to south, the diurnal cycle progressively flattens, and the magnitudes of the high–low bars decrease. The semidesert

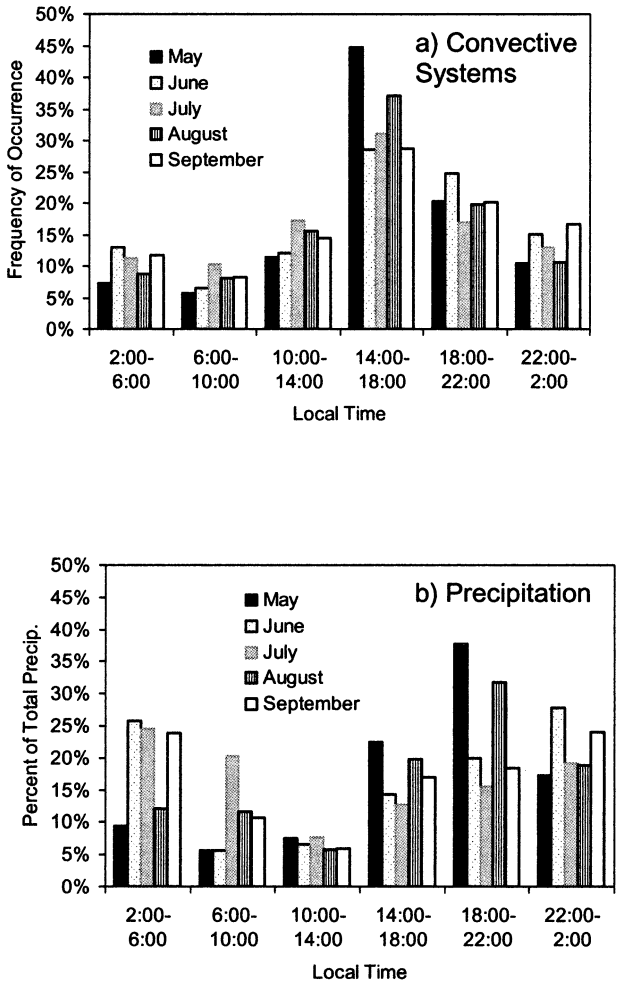

FIG. 7. (a) The frequency of occurrence of convective systems and (b) percent of total precipitation occurring in 4-h local time blocks by month.

and savanna zones have two pronounced peaks, with one peak in the early evening and the second in the early morning. Diurnal cycles with two peaks were also observed in studies of precipitation in Niger by Shinoda et al. (1999) and Mathon et al. (2002). In contrast to the semidesert and savanna zones, the forest zone's diurnal cycle has only one peak, peaking at 1800–2200 LT. The value in the 1800–2200 LT block is only slightly higher than the value in the 2200–0200 LT block, compared to the sharp decreases in the 2200–0200 LT blocks of the other two zones.

The comparison of wetter versus drier years in the previous section revealed differences in the frequency of organized systems but not in the size and intensity distribution of the convective system population as a whole. Figures 7 and 8 are compiled from all 4 yr of data, thereby combining the wetter and drier years. In Fig. 9, each year is plotted separately to see if the differences in system frequency might result in different diurnal cycles. The diurnal cycles of the wetter years are distinctly different from the drier years. The wetter years have only one peak, analogous to the forest zone cycle, and the drier years have two peaks, analogous to the semidesert and savanna zone cycles. The diurnal cycles of the wetter years peak at 2200–0200 LT, one box later than the first peak in the drier years. The wetter years have more pronounced single peaks than the forest zone diurnal cycle in Fig. 8c where the values for 1800–2200 and 2200–0200 LT are similar. The shape and magnitude of the peaks in the drier years most closely resemble the savanna zone's cycle. The diurnal cycle for 2000 does not decrease as sharply between 1800–2200 and 2200–0200 LT as in 2001. It is worth recalling that 2000 also had more precipitation than 2001 (Table 2).

6. Discussion

Figures 7–9 demonstrate variability in the diurnal cycle intraseasonally, regionally, and interannually, respectively. The evidence presented in section 4 pointed to the frequency of convective systems as being the principal difference between the wetter years (1998 and 1999) and the drier years (2000 and 2001) in this study. This section attempts to make some links between convective population characteristics and the variability of the diurnal cycle.

The diurnal cycles of precipitation in Figs. 7–9 do not distinguish among the contributions made by convective systems defined as young/weak, mature, or decaying/stratiform. In Fig. 10a, the frequency of occurrence of each system type has its own diurnal cycle. The plots of the young/weak and mature convective systems are similar to each other, with peaks greater than 30% at 1400–1800 LT, and comparable to Fig. 7a. The decaying/stratiform plot peaks at 0200–0600 LT, and the plot of the organized convective systems has a bimodal shape most similar to the savanna diurnal cycle in Fig. 8b. In Fig. 10b, the 50th percentile for total system area rises slightly from 1400–1800 to 1800–2200 LT then levels off. The 90th percentile rises continuously from 1400–1800 to 0200–0600 LT, with the largest increase between 1400–1800 and 1800–2200 LT. It appears from Fig. 10 that the organized convective systems reach maturity after 1800 LT with the largest ones lasting until early morning and that the frequency of organized convective systems is the principal control on the diurnal cycle of precipitation. From June to July, the number of organized convective systems in the forest zone declines by 2% but there is a 10% zonal average reduction in precipitation, with reductions as large as 20% in individual latitude–longitude boxes. A small percentage increase in the number of organized convective systems can be expected to produce a much larger percentage increase in precipitation in the late-evening/early-morning time blocks. The midafternoon time block is likely to increase also but less dramatically.

Figure 7 depicts the seasonal variability of the diurnal

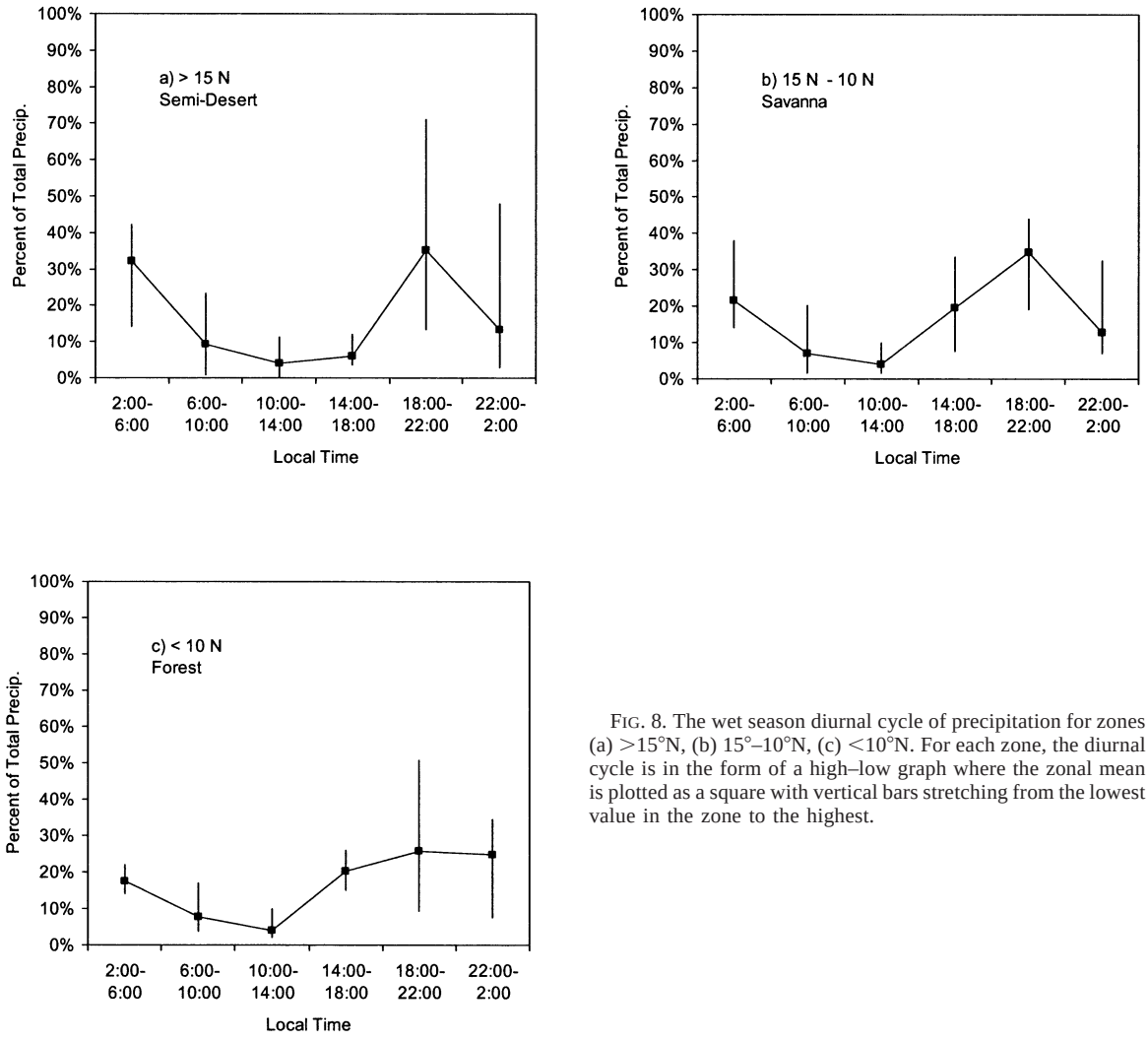

FIG. 8. The wet season diurnal cycle of precipitation for zones (a) >15°N, (b) 15°–10°N, (c) <10°N. For each zone, the diurnal cycle is in the form of a high–low graph where the zonal mean is plotted as a square with vertical bars stretching from the lowest value in the zone to the highest.

cycle for the entire study area, and Fig. 8 contains the diurnal cycles of the three land cover zones for the entire wet season. The high–low bars of Fig. 8 imply seasonal variability, and the bars in Fig. 7 encompass zonal and meridional variability. None of the diurnal cycles in Fig. 7 precisely replicate any of the diurnal cycles of the zones in Fig. 8, although the broad peaks from 2200–0600 LT in June, July, and September in Fig. 7 coincide with the location of the ITCZ and a high frequency of organized convective systems in the savanna zone. The rest of the discussion will thus center on organized convective systems and their possible roles in diurnal cycle variability.

May and August have conspicuous peaks at 1800–2200 LT. In May the ITCZ is in the forest zone, in August, the semidesert zone. Two possibilities for the May/August diurnal cycles come to mind, a greater contribution from shorter-lived organized convective systems and from convective systems originating in the late afternoon (1400–1800). Rowell and Milford (1993) show that the mean lifetime of squall lines decreases both north and south of the zone (10°–15°N) defined as the savanna zone in this study, although the decrease in mean lifetime is greater north of 15°N than south of 10°N. From a dynamical perspective it is worth noting that in the summer, the climatological axis of the African easterly jet is in the savanna zone, increasing the chances a propagating convective system will be long-lived (Rotunno et al. 1988; Cook 1999). Since long-lived convective systems spread precipitation over a larger span of time and space, the higher frequency of long-lived convective systems in the savanna zone would minimize zonal differences. In addition to longevity, the size of an organized convective system would affect how it spreads precipitation over time and space, so it is worth noting that organized convective systems tend to be larger in the forest zone than in the other zones (size distributions by zone not shown).

Small convective systems make a nonnegligible contribution to precipitation in the semidesert forest zone in May and in the forest zone in August. Mohr et al. (2003) simulated convective systems in forest, savanna,

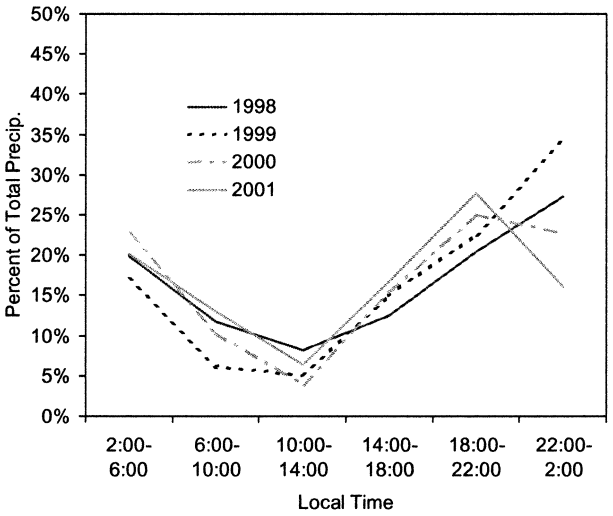

FIG. 9. Diurnal cycles of precipitation for each year in the study database for the entire study area. Wetter years (1998 and 1999) use black lines, and drier years (2000 and 2001) use gray lines.

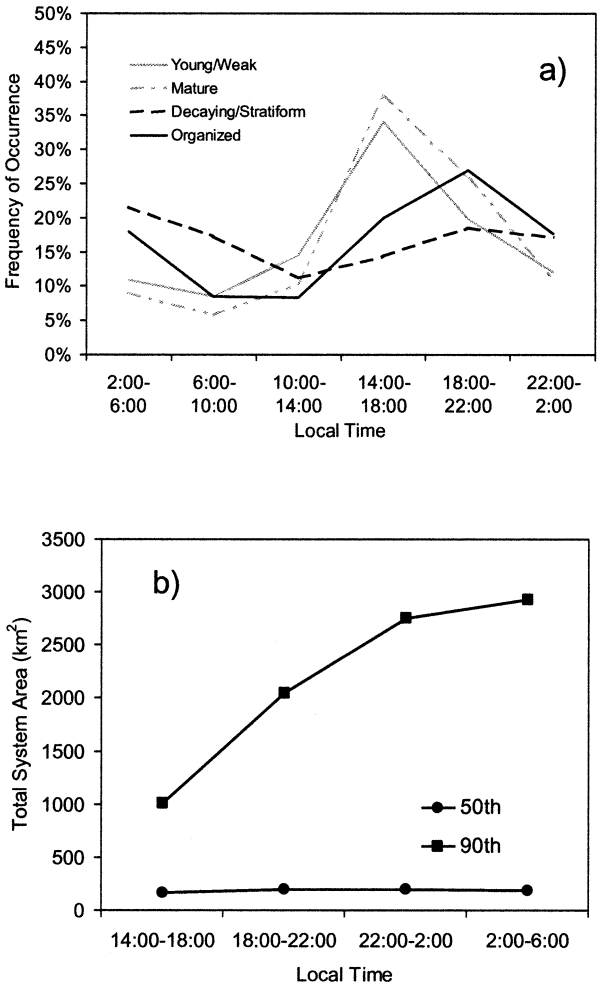

FIG. 10. (a) The frequency of occurrence by system type vs time. (b) The 50th and 90th percentiles for total system area of convective systems in the study database, sorted by selected time blocks.

and semidesert environments, demonstrating that land surface conditions influenced the timing and intensity of modeled convective lines. The boundary layer of the forest environment was moister (2–3 g kg^{-1}) and shallower (by one model layer) than the savanna environment. Heavy rain from both small and organized convective systems developed several hours earlier in the day in the forest than in the savanna. In Rowell and Milford's study, short-lived (<4 h) squall lines typical of the semidesert zone originated and dissipated mainly within the 1800–2200 LT time block. While the forest zone appears to dominate May's diurnal cycle, August weighs the contributions from small convective systems and shorter-lived organized convective systems in the forest and semidesert versus longer-lived organized convective systems in the savanna. The former would have the effect of skewing August's peak toward earlier in the evening compared to July or September.

Comparing the magnitudes of seasonal changes to zonal variability in the diurnal cycle, the savanna and forest zones have seasonal changes of about 10% and zonal variability of about 1%. Both the zonal and seasonal differences in the semidesert zone are about 10%. Topography (Fig. 1b) has been a major player in previous studies (Rowell and Milford 1993; Hodges and Thorncroft 1997) of the life cycle organized convective systems thus making it important in the zonal variability of the diurnal cycle as well. In Rowell and Milford, organized convective systems north of 15°N originate near the Aïr Mountains or the northern branch of the Niger River, in the early evening and often decaying soon afterward. Between 10°–15°N, organized convective systems tend to generate near the Jos Plateau in the late afternoon, decaying sometime around midnight. Other triggering sites include the Dhafur Mountains and the Guinea Highlands (Hodges and Thorncroft 1997). The Cameroon Highlands is the most likely generation region for organized convective systems south of 10°N. For the highly variable semidesert zone, Fig. 11 illustrates the differences in the diurnal cycles for the latitude–longitude box containing the Aïr Mountains and the two boxes west of it. Progressively westward from the Aïr Mountains, the value in the 1800–2200 LT box decreases while the value in the 0200–0600 LT box increases. Note that individual boxes have more lopsided two-peak diurnal cycles than the composite cycle in Fig. 8a. Because the total amount of precipitation in the semidesert zone is considerably less than the zones south of it, when even a few long-lived organized convective systems reach the western boxes in the early morning, they can contribute a large enough share of precipitation to create the second peak in the composite semidesert diurnal cycle. In the savanna zone, there is a similar but more subdued shift from a peak at 1800–2200 LT to a peak at 0200–0600 LT west of the Jos Plateau.

Using the 30-dBZ heights from the TRMM PR, Nes-

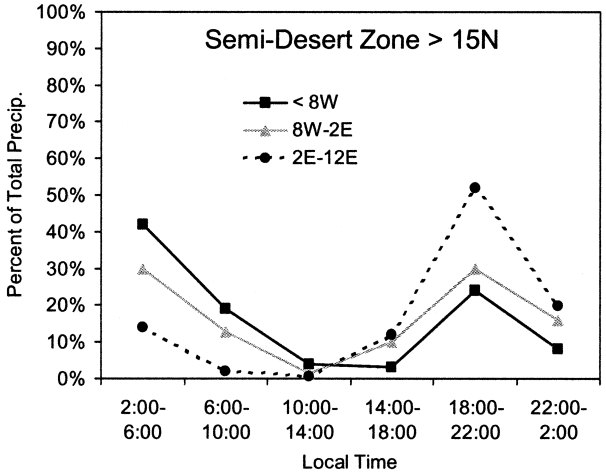

FIG. 11. The diurnal cycles of precipitation for three selected lat–lon boxes within the semidesert zone. The 2°–12°E box contains the Aïr Mountains, a principal generation area for organized convective systems in this zone.

bitt and Zipser (2003) show how storm intensity changes diurnally. The shape of the bimodal savanna and semidesert diurnal cycles in Figs. 8 and 10a parallel the documented life cycle of organized systems in the Sahel (e.g., Rowell and Milford 1993; Hodges and Thorncroft 1997). The greatest share of intense convective precipitation occurs after genesis (1800–2200 LT), and the greatest share of stratiform precipitation occurs before lysis in the early morning (0200–0600 LT). The broad peak of the forest zone reflects a greater contribution from small convective systems and differences in the life cycles of organized convective systems in the more humid environment south of the African easterly jet. The broad peaks of the monthly diurnal cycles of Fig. 7 would then be the result of merging the contributions of all zones. The late, single peak of the wetter years in Fig. 9 reflects increases in convective systems of all sizes but particularly of organized convective systems. Even after averaging, it is apparent that the life cycle of organized convective systems shifts the peak in precipitation to later in the evening than the peak in the frequency of all convective systems. The evidence of this study implies that variability in the diurnal cycle of sub-Saharan Africa can be largely attributed to variability in the frequency and life cycle of organized convective systems and thus the physical and dynamical factors responsible for their development.

7. Summary

This study used 4 yr of TRMM data (1998–2001) to analyze the relationship between variability in the diurnal cycle of precipitation and the nature of the convective system population of sub-Saharan Africa. The study database was derived from four wet seasons, May–September, of 85-GHz data from the TRMM Microwave Imager. Convective systems were defined from contiguous 85-GHz pixels of 255 K or colder. Using a discrimination algorithm developed by Prabhakara et al. (2000), pixels were classified as convective (young/weak, mature, or decaying) or stratiform cloud from the spatial temperature gradients within each convective system. Information on all convective systems detected such as location and size was stored in a relational database. sub-Saharan Africa was divided into 15 boxes at 10° × 5° and three 5° zones containing a principal land cover, semidesert (>15°N), savanna (10°–15°N), and forest (<10°N). These divisions were intended to detect the influences of topography and land cover.

The study time period contained two wetter than average years (1998, 1999) and two drier than average years (2000, 2001). The only population characteristic distinguishing the wetter years from the drier years was frequency of occurrence of convective systems because the size and intensity distributions for the wetter and drier years were virtually identical. The wetter years had about 10% more convective systems than the drier years. Even if large and/or intense convective systems represented the same percentage of the convective system population in both the wetter years and drier years, there were more of them in the wetter years. In a multiyear study of West African precipitation datasets, Sealy et al. (2003) attribute precipitation anomalies to variations in stratiform rain. A reduction in the frequency of organized convective systems necessarily means a proportionately larger reduction in the amount of stratiform rain. At the upper end of the logarithmic size distribution, the fraction of stratiform cloud increases significantly, and the increases in total system area are principally from increases in stratiform cloud area (cf. Fig. 3). Extrapolating from the study database, a 1%–2% reduction in the number of organized convective systems would produce as much as a 10%–20% reduction in precipitation.

From north to south, the mean wet season diurnal cycle of precipitation evolves from a bimodal, highly variable diurnal cycle north of 15°N to a unimodal, much less variable diurnal cycle south of 10°N. Both zonal variability and the seasonal cycle produced changes on the order of 10% in the diurnal cycle. These changes were most noticeable in certain time blocks (1800–2200 and 0200–0600 LT) and in the semidesert zone north of 10°N. The characteristics of the organized convective system population seem to be more important to understanding the variability of the diurnal cycle than the characteristics of the general convective system population. The frequency of organized convective systems is strongly tied to the seasonal cycle and will vary from year to year to a greater degree than the frequency of all convective systems. The influence of small convective systems is limited, applying mainly to certain months (e.g., May) and certain areas (e.g., the forest zone). The organized convective system is the integration of physical (topography and land cover) and dynamical (e.g., African easterly jet, monsoon circulation)

factors at a near-GCM grid scale. This should allow researchers to focus on a small subset of the convective system population and their particular environments to explain most of the variability in precipitation cycles.

Previous work on diagnosing the West African diurnal cycle compiled a single representative diurnal cycle. This study reveals that there are different diurnal cycles for each of the three 10° zones south of the Sahara Desert. There are also differences interannually between the diurnal cycles of wetter and drier years. The regional and temporal variability of diurnal cycles in sub-Saharan Africa may give some pause to dynamical modelers, but improved simulation of organized convective systems should alleviate this problem. Detailed process studies of land–atmosphere interaction at a variety of scales coupled with ground and satellite observations should help improve the description of the key physical processes and variables by which the African land surface affects the development of organized convective systems.

Acknowledgments. TRMM is cosponsored by NASA and NASDA, the Japanese space agency. Special thanks to C. Prabhakara and Bob Iacovazzi for helping me with their discrimination algorithm and to the hard-working staff at the NASA Goddard DAAC for making TRMM data easily available to researchers. I had valuable discussions with Greg Jenkins, Andy Negri, Doug Parker, and Chris Thorncroft during this research. The comments of my generous anonymous reviewers helped me polish this manuscript. I received financial support from NSF Grant 0215413.

REFERENCES

Bailey, R. C., 1998: *Ecoregions: The Ecosystem Geography of the Oceans and Continents.* Springer-Verlag, 176 pp.

Cook, K. H., 1999: Generation of the African easterly jet and its role in determining West African precipitation. *J. Climate,* **12,** 1165–1184.

Desbois, M., T. Kayiranga, B. Gnamien, S. Guessous, and L. Picon, 1988: Characterization of some elements of the Sahelian climate and their interannual variations for July 1983, 1984, and 1985 from the analysis of METEOSAT ISCCP data. *J. Climate,* **1,** 867–904.

Duvel, J. P., 1989: Convection over tropical Africa and the Atlantic Ocean during northern summer. Part I: Interannual and diurnal variations. *Mon. Wea. Rev.,* **117,** 2782–2799.

Hodges, K. I., and C. D. Thorncroft, 1997: Distribution and statistics of African mesoscale convective weather systems based on the ISCCP Meteosat imagery. *Mon. Wea. Rev.,* **125,** 2821–2837.

Kummerow, C., W. Barnes, T. Kozu, J. Shiue, and J. Simpson, 1998: The Tropical Rainfall Measuring Mission (TRMM) sensor package. *J. Atmos. Oceanic Technol.,* **15,** 809–817.

Laing, A., and J. M. Fritsch, 1993: Mesoscale convective complexes in Africa. *Mon. Wea. Rev.,* **121,** 2254–2263.

Machado, L. A. T., J. P. Duvel, and M. Desbois, 1992: Structural characteristics of deep convective systems over tropical Africa and the Atlantic Ocean. *Mon. Wea. Rev.,* **120,** 392–406.

——, ——, and ——, 1993: Diurnal variations and modulation by easterly waves of the size distribution of convective cloud clusters over West Africa and the Atlantic Ocean. *Mon. Wea. Rev.,* **121,** 37–49.

Mathon, V., and H. Laurent, 2001: Life cycle of Sahelian mesoscale convective cloud systems. *Quart. J. Roy. Meteor. Soc.,* **127,** 377–406.

——, ——, and T. Lebel, 2002: Mesoscale convective system rainfall in the Sahel. *J. Appl. Meteor.,* **41,** 1081–1092.

Mohr, K. I., and E. J. Zipser, 1996: Mesoscale convective systems defined by their 85-GHz ice scattering signature: Size and intensity comparison over tropical oceans and continents. *Mon. Wea. Rev.,* **124,** 2417–2437.

——, J. S. Famiglietti, and E. J. Zipser, 1999: The contribution to tropical rainfall with respect to convective system type, size, and intensity estimated from the 85-GHz ice-scattering signature. *J. Appl. Meteor.,* **38,** 596–606.

——, R. D. Baker, W.-K. Tao, and J. S. Famiglietti, 2003: The sensitivity of West African convective line water budgets to land cover. *J. Hydrometeor.,* **4,** 62–76.

Negri, A. J., T. L. Bell, and L. Xu, 2002: Sampling of the diurnal cycle of precipitation using TRMM. *J. Atmos. Oceanic Technol.,* **19,** 1333–1344.

Nesbitt, S. W., and E. J. Zipser, 2003: The diurnal cycle of rainfall and convective intensity according to three years of TRMM measurements. *J. Climate,* **16,** 1456–1475.

——, ——, and D. J. Cecil, 2000: A census of precipitation features in the Tropics using TRMM: Radar, ice scattering, and lightning observations. *J. Climate,* **13,** 4087–4106.

Nicholson, S. E., 1993: An overview of African rainfall fluctuations of the last decade. *J. Climate,* **6,** 1463–1466.

Peterson, W. A., and S. A. Rutledge, 2001: Regional variability in tropical convection: Observations from TRMM. *J. Climate,* **14,** 3566–3586.

Prabhakara, C., J. R. Iacovazzi, J. A. Weinman, and G. Dalu, 2000: A TRMM microwave radiometer rain rate estimation method with convective and stratiform discrimination. *J. Meteor. Soc. Japan,* **78,** 241–258.

Rotunno, R., J. B. Klemp, and M. L. Weisman, 1988: A theory for strong, long-lived squall lines. *J. Atmos. Sci.,* **45,** 463–485.

Rowell, D. P., and J. R. Milford, 1993: On the generation of African squall lines. *J. Climate,* **6,** 1181–1193.

Sealy, A., G. S. Jenkins, and S. C. Walford, 2003: Seasonal/regional comparisons of rain rates and rain characteristics in West Africa using TRMM observations. *J. Geophys. Res.,* **108D,** 4036–4057.

Shinoda, M., T. Okatani, and M. Saloum, 1999: Diurnal variations of rainfall over Niger in the West African Sahel: A comparison between wet and drought years. *Int. J. Climatol.,* **19,** 81–94.

Spencer, R. W., H. M. Goodman, and R. E. Hood, 1989: Precipitation retrieval over land and ocean with the SSM/I: Identification and characteristics of the scattering signal. *J. Atmos. Oceanic Technol.,* **6,** 254–273.

Taylor, C. M., and T. Lebel, 1998: Observational evidence of persistent convective-scale rainfall patterns. *Mon. Wea. Rev.,* **126,** 1597–1607.

Toracinta, E. R., K. I. Mohr, E. J. Zipser, and R. E. Orville, 1996: A comparison of WSR-88D reflectivities, SSM/I brightness temperatures, and lightning for mesoscale convective systems in Texas. Part I: Radar reflectivity and lightning. *J. Appl. Meteor.,* **35,** 902–918.

Yang, G.-Y., and J. Slingo, 2001: The diurnal cycle in the Tropics. *Mon. Wea. Rev.,* **129,** 784–801.